Uncovering Hemispheric Asymmetry and Directed Oscillatory Brain-Heart Interplay in Anxiety Processing: An fMRI Study

Ameer Ghouse, *Member, IEEE*, Gert Pfurtscheller, *Senior Member, IEEE*, Gerhard Schwarz, and Gaetano Valenza, *Senior Member, IEEE*

***Abstract*— Brain-heart interactions (BHI) are critical for generating and processing emotions, including anxiety. Understanding specific neural correlates would be instrumental for greater comprehension and potential therapeutic interventions of anxiety disorders. While prior work has implicated the pontine structure as a central processor in cardiac regulation in anxiety, the distributed nature of anxiety processing across the cortex remains elusive. To address this, we performed a whole-brain-heart analysis using the full frequency directed transfer function to study resting-state spectral differences in BHI between high and low anxiety groups undergoing fMRI scans. Our findings revealed a hemispheric asymmetry in low-frequency interplay (0.05 Hz - 0.15 Hz) characterized by ascending BHI to the left insula and descending BHI from the right insula. Furthermore, we provide evidence supporting the "pacemaker hypothesis", highlighting the pons' function in regulating cardiac activity. Higher frequency interplay (0.2 Hz - 0.4Hz) demonstrate a preference for ascending interactions, particularly towards ventral prefrontal cortical activity in high anxiety groups, suggesting the heart's role in triggering a cognitive response to regulate anxiety. These findings highlight the impact of anxiety on BHI, contributing to a better understanding of its effect on the resting-state fMRI signal, with further implications for potential therapeutic interventions in treating anxiety disorders.**

***Index Terms*— Functional magnetic resonance imaging, brain modeling, psychiatry, system dynamics.**

Manuscript received 18 September 2023; revised 16 February 2024; accepted 3 May 2024. Date of publication 15 May 2024; date of current version 24 May 2024. This work was supported in part by European Commission Horizon 2020 Research and Innovation Program through the Project EXPERIENCE under Grant 101017727 and in part by Italian Ministry of Education and Research (MIUR) in the Framework of the FoReLab Project (Departments of Excellence). *(Corresponding authors: Ameer Ghouse; Gaetano Valenza.)*

This work involved human subjects or animals in its research. Approval of all ethical and experimental procedures and protocols was granted by the Local Ethics Committee at the University of Graz under Application No. GZ. 39/75/63 ex 2013/14.

Ameer Ghouse and Gaetano Valenza are with the Neuro- Cardiovascular Intelligence Laboratory, Research Center "E. Piaggio" & Department of Information Engineering, School of Engineering, University of Pisa, 56126 Pisa, Italy (e-mail: a.ghouse@studenti.unipi.it; gaetano.valenza@unipi.it).

Gert Pfurtscheller is with the Institute of Neural Engineering, BCI-Laboratory, Graz University of Technology, 8010 Graz, Austria.

Gerhard Schwarz is with the Department of Anaesthesiology and Intensive Care Medicine, Medical University of Graz, 8010 Graz, Austria.

Digital Object Identifier 10.1109/TNSRE.2024.3401577

I. Introduction

THE experience of anxiety is not only a mental phenomenon, but also a physiological one [1], [2], [3]. It is often characterized by feelings of apprehension, worry, and fear [2]. Anxiety can trigger a range of bodily responses, including increased heart rate, rapid breathing, dry mouth, dizziness, and muscle tension [3], [4], [5], [6]. One important proxy of cardiovascular dynamics is heart rate variability (HRV) series, which refers to the variation in time between successive heartbeats. HRV has been shown to be a sensitive indicator of the balance between the sympathetic and parasympathetic branches of the autonomic nervous system, and to be linked to anxiety-related responses [17], [18], [19]. These bodily responses are regulated by the autonomic nervous system, a complex network of nerves that controls involuntary functions such as heart rate, blood pressure, and digestion [7]. Research has highlighted the bidirectional signaling between the brain and the autonomic nervous system in regulating anxiety [8], [9], [10], [11]. In particular, the vagus nerve, which connects the brain and the autonomic nervous system, plays a critical role alongside the pontine structure in modulating anxiety-related responses. Still, little is understood about the distributed brain-heart interactions (BHI) across the cortex. Understanding the physiology of interactions between the brain and body during anxiety regulation is essential for characterizing the physiological networks that sustain emotional and mood states, as well as for developing effective interventions that target the autonomic nervous system, such as biofeedback and heart rate variability training [36].

Anxiety can be particularly acute for individuals undergoing a magnetic resonance imaging (MRI) scan [12], [13], [14]. The confined space, loud noise, physical discomfort, concern about harm, fatigue from examination duration, and unfamiliar environment can all trigger anxiety-related bodily responses [9], [15], [16], such as increased heart rate and sweating. Understanding the advent of anxiety in MRI imaging is fundamental in abetting claustrophobic conditions in clinical settings. A systematic meta-analysis revealed in approximately 12 out of 1000 people (1 - 2 %) scanned in an MRI machine succumbed to a claustrophobic reaction and demanded a premature termination of the scan [41]. Such abortions not only raise the costs of fMRI examinations, but also delay

essential diagnoses for patients. In this respect, quantifying MRI-related anxiety levels, like in [42], is of interest, where there is first an initial increase of anxiety, followed by a subsequent decrease in the middle of the scanning, culminating in a final increase of anxiety towards the end of scanning.

The pons and amygdala are two important regions of the brain that are known to be instrumental for emotional and anxiety processing [1], [20], [21], [22], [28], [29], [30]. The amygdala is involved in the detection and processing of emotionally salient information [23], [24], while the pons, a structure that runs rostro-caudally anterior to the cerebellum [25], is responsible for regulating autonomic functions such as heart rate, blood pressure, and respiration [5], [26] with specific nuclei such as the locus coeruleus and parabrachial brachial nucleus that affect the arousal and the cardiovascular system [27]. Though the exact mechanism by which anxiety is elicited by the pons is not well understood, specific nuclei, namely the locus coeruleus, has been shown to be involved in arousal through its release of the neurotransmitter norepinephrine into the brain for anxiety regulation [31], as well as receiving input from the vagus nerve involved in parasympathetic regulation of visceral signals [32], [33]. Furthermore, previous studies performed stimulations to identify the direct interactions between the midbrain, comprising structures such as the amygdala and hippocampus, and the heart, both in humans and in rodents [34], [35].

It has been shown that cortical areas also play a role in anxiety processing. There is evidence for the posterior insular cortex as a potential mediator of bottom-up cardiac interoceptive processing, and that inhibition of this brain region attenuates anxiety-like behavior induced by cardiac pacing [39]. Indeed, the insular cortex has been shown to be tightly interwoven with the autonomic system, demonstrating hemisphere specific ascending and descending streams of interactions [8], [40]. These findings suggest that there is a close relationship between cardiac interoceptive processing and anxiety-related behavior, and that the posterior insular cortex particularly may be a target for addressing anxiety disorders.

Given these previous findings and implications, single participant fMRI scans can provide a new methodological framework to understand the effects of anxiety on the brain-heart axis. Does coupling between the heart and brain signals as measured in an fMRI scan differ when a participant is undergoing levels of high anxiety (beginning of fMRI scan) compared to low anxiety (middle of fMRI scan)? If so, are there differences in coupling patterns involving the insular cortex, pons, amygdala, or other brain regions involved in interoception and anxiety regulation? The body and the brain must be considered together to understand the origins of emotional states [43], demanding analysis of coupling between the heart and the whole brain, as opposed to isolated regions, which may subsequently be important in elucidating the complex interplay between the body and the brain in emotional processing. Therefore, exploring the causal coupling between the heart and the whole brain may provide a more comprehensive understanding of the neurobiological mechanisms underlying anxiety and other affective states. Developing a methodological framework for studying these effects would allow for a more comprehensive understanding of the neural substrate underlying anxiety and how they may be related to interoceptive processing in the body.

Therefore, to investigate the links between the heart and the brain in individuals with high and low anxiety, we here propose a methodological framework relying on full frequency directed transfer function (ffDTF) [44]. Granger causality is a statistical technique that allows inference of causal relationships between time series data [45], such as the heart rate and brain signals acquired during fMRI scans. The ffDTF is a variant of Granger causality that allows for the detection of causal relationships at multiple frequencies [44], [46], providing a more comprehensive picture of the interactions between the heart and the brain. To parcellate the brain into meaningful regions of interests for brain-heart interplay (BHI) analysis, we utilized the AAL2 atlas [47]. To specify pons specific structures in the upper brainstem on this atlas, we used nearby anterior cerebellar regions of interest such as vermis III to V, cerebellar lobules III to V, and posterior cerebellar regions of interests such as cerebellar lobules IX and X. By applying the ffDTF with multiple comparisons corrections to data obtained from subjects entering an MRI machine with either high or low anxiety, we aimed to uncover differences in the strength of ascending (heart to brain) and descending (brain to heart) causal interactions in these two groups. The fMRI-based proposed methodology may in turn reveal potential neurobiological markers of anxiety and inform the development of targeted interventions for anxiety disorders.

II. Methods and Materials

A. Study Approval

The protocol of the study was approved by the local Ethics Committee at the University of Graz (number: GZ. 39/75/63 ex 2013/14), and all participants provided written informed consent. Our research adhered to the ethical standards outlined in the 1964 Declaration of Helsinki.

B. Study Design

To study anxiety processing during scanning in healthy fMRI participants, it is necessary to first categorize individuals into groups based on their anxiety levels. This requires defining two groups: one with high anxiety (HA) and another with low or no anxiety (LA). The foundation for this categorization was established through a fMRI study that included four resting states, recording of respiration and ECG during scanning, as well as a questionnaire administered within the scanner.

C. Experiment Paradigm

The study employed four resting states each lasting 5 minutes embedded in a larger 45 minute recording session. A state anxiety score was evaluated through within-scanner questionnaires completed before first and third resting state session, and after the second and fourth resting state session. The questionnaires took approximately 5 minutes to fill out. The state-trait anxiety and depression inventory (STADI was used

to measure state anxiety, with the items displayed on a screen within the scanner and answered via a trackball.

To further elaborate, our categorization of state anxiety was grounded in both theoretical assumptions and practical considerations. Initially, we specifically chose cases that exhibited successful anxiety regulation, as evidenced by a linear decrease during resting phases. This approach ensured that all individuals demonstrated a healthy response trajectory, aligning with what could be reasonably expected (habituation). Subsequently, the classification into high and low anxiety categories relied on normative values obtained from the questionnaire. It is important to note that the normative mean of the state anxiety scale is 16.68, and we made the decision to include cases both below and above this mean. A score of 15 (LA) corresponds to a percentile rank of 48%, indicating that approximately half of the normative sample displayed values equal to or lower than 15. Conversely, a score of 16 has a percentile rank of 64%. Therefore, we were able to effectively identify anxiety scores that were relatively low and high, resulting in equal sample sizes for both categories. Additional information can be found in [29].

D. Participants

The data were taken from an openly available dataset (at https://osf.io/vdkjs/) collected from a previous fMRI study involving 23 participants (12 females, 11 men) aged between 19 to 34 years, of whom a total of 22 subjects were right handed. The participants had no prior experience with MRI and had no history of neurological or psychiatric disorders.

The participants were instructed to keep their eyes open and to focus on a black screen during the resting state. Out of the 23 participants, 14 demonstrated successful anxiety processing, with a decline in anxiety from the first to the last resting state [29]. Four participants exhibited prevailing or increasing anxiety, and no clear pattern was found in five participants. One participant had technical issues with the scanning sequence, and four participants had unusable ECG recordings, resulting in their exclusion from further analysis. In a previous study, anxiety processing was studied for these 14 subjects [29], where there were significantly higher anxiety differences from initial resting state (HA14: 21.9 ± 4.1) to the last resting state (LA14: 12.4 ± 1.5).

E. Physiological Signal Recording and RRI Time Courses

Inside the scanner, both the electrocardiogram (ECG) and respiration were recorded at a sampling rate of 400 Hz. The RRI time series were obtained by performing QRS detection and computation using the fMRI plug-in for EEGLAB [48] To enhance the RRI signals, the Kubios HRV Premium Package [49] was utilized. For more comprehensive information, refer to [50].

F. Resting State fMRI and ROI Selection

The study utilized a 3 T scanner (Magneton Skyra, Siemens, Erlangen, Germany) to obtain functional images. The images were acquired using a multiband GE-EPI sequence [51], which allowed for a simultaneous six-band acquisition. The imaging parameters were TE/TR = 34/871 ms, 52^o flip angle, $2 \times 2 \times 2mm^3$ voxel size, 66 contiguous axial slices (11×6), acquisition matrix of 90×104, and a FOV of $180 \times 208mm^2$. Time courses for 116 ROIs of interest were extracted using the AAL2 atlas [47]. Analysis epochs of 53 seconds were used. For additional information, please refer to [30].

G. Computing of Causal Coupling and Statistic

The Directed Transfer Function (DTF) is a measure of directional influence between two signals, which is often used in the context of time-series analysis [46]. In the field of neuroscience, DTF can be used to estimate the causal interactions between different regions of the brain, based on their time-series recordings [52]. The novelty of this study is incorporating R-R intervals as an auxiliary signal, as done in previous work in [28], but furthermore considering whole brain analysis to assess brain-heart interactions (BHI) beyond only isolated regions.

To calculate the DTF for whole brain analysis, we can use a k-channel Granger Causality (GC) model, which is a variant of the traditional GC model that allows for multiple channels of input and output. The k-channel GC model estimates the causal interactions between all pairs of channels (AAL2 brain parcels and R-R Intervals) simultaneously, by fitting a multivariate autoregressive (MVAR) model to the time-series data.

The MVAR model is typically specified as follows:

$$X(t) = \sum_{i=1}^{p} A(i)X(t-i) + E(t), \tag{1}$$

where $X(t)$ is a k-dimensional vector of time-series measurements at time t, $A(i)$ is a $k \times k$ matrix of autoregressive coefficients for lag i, and $E(t)$ is a k-dimensional vector of residual errors at time t. The order p of the model determines the number of lagged time points used in the regression. We select the appropriate order p for the MVAR model based on the Akaike Information Criterion (AIC).

Once the MVAR model has been estimated, a Fourier transform can be utilized to convert from time-domain to frequency domain:

$$A(f)X(f) = E(f) \tag{2}$$

where the components of $A(f)$ are:

$$A(f) = -\sum_{i=0}^{p} A(i)e^{-j2\pi fi} \tag{3}$$

where A(0) is the identity matrix I. Eq. 2 can be manipulated to obtain a transfer function $H(f)$ of the inputs $E(f)$ to outputs $X(f)$ as follows:

$$X(f) = A^{-1}(f)E(f) = H(f)E(f) \tag{4}$$

Once $H(f)$ is obtained, we can compute the DTF using the following formula:

$$DTF_{ij}(f) = \frac{|H_{ij}(f)|^2}{\sum_{n=1}^{k} |H_{in}(f)|^2}, \tag{5}$$

where $H_{ij}(f)$ is the transfer function from channel j to channel i at frequency f, and k is the total number of channels.

The DTF can be normalized for a band of interest to obtain the full frequency DTF (ffDTF) [44]:

$$ffDTF_{ij}(f) = \frac{|H_{ij}(f)|^2}{\sum_f \sum_{n=1}^{k} |H_{in}(f)|^2}, \quad (6)$$

The ffDTF indicates the causal impact from channel j to channel i at a given frequency f in comparison to the overall impact from all channels. To measure coupling strength, ffDTFs were combined across frequency bands of interest, namely LF (0.05–0.15 Hz), IMF (0.1–0.2 Hz) and HF (0.2-0.4 Hz), and averaged over epochs. This approach enabled the determination of $C_{ij} = \sum_{f=f_{low}}^{f_{high}} ffDTF(f)$, which reflects the strength of coupling between signals j and i in the selected frequency range, as calculated from the ffDTF. We measured the ffDTF for each of the 53 second epochs extracted for each resting state session. Then, prior to statistical analysis, we computed the mean value of the ffDTF over the epochs for each session before performing statistical analysis to account for nonstationarity of the resting state signal [53].

H. Statistical Analysis

To obtain significance statistics, we performed bootstrapped permutation analysis as described in [29]. To paraphrase, the statistical analysis aimed to detect significant differences in average coupling values C_{ji} between high arousal (HA) and low arousal (LA) samples in selected frequency bands using the bootstrap approach. As the theoretical distribution of C_{ji} is unknown, we compared its values with surrogate data distributions obtained through bootstrapping. The study focused on three frequency bands: 0.05–0.15 Hz, 0.1–0.2 Hz, and 0.2–0.4 Hz. The null hypothesis (H_0) states that there is no difference ($D_{ji} = 0$) between HA and LA samples, whereas the alternative hypothesis (H_1) states that a difference ($D_{ji} \neq 0$) exists, where $D_{ji} = C_{ji}^{HA} - C_{ji}^{LA}$. To obtain the distribution of D_{ji} under the null hypothesis, we followed these bootstrap steps:

1) We created a common pool of subjects from both samples.
2) We randomly selected (with replacements) two subsets of 14 subjects (with 8 epochs each) and marked them as type 1 and type 2.
3) We computed $D_{jiboot} = C_{jitype1} - C_{jitype2}$ for each i, j.
4) We repeated steps 1–3 for 10,000 times and saved each obtained D_{jiboot} value. This gives an empirical distribution of D_{ji} to use for obtaining p-values.
5) For robust inferences, we identified the connections for which the original values of connectivity difference D_{ji} were significant after correcting for multiple comparisons using the false discovery rate according to the Bejamini-Horschberg procedure [54] with $q = 0.05$.

I. Data and Code Availability

All code used to obtain the results in this study can be found at https://github.com/lemiceterieux/Brain-Heart-Interplay-in-Anxiety-Processing. Furthermore, ROI parcellated fMRI and R-R interval data is available publicly at https://osf.io/vdkjs/.

III. Results

The present study investigated BHI during anxiety processing using ffDTF applied to synchronized fMRI and cardiac signal (RRI) data, with a subset of results seen in table I. Among the 116 regions of interest (ROIs) examined, only a small subset displayed statistical significance. Specifically, these included ROIs located in the upper brainstem (pons), such as CER4_5, CER8, CER9, (left side), and CER9, CER10 (right side); ROIs within the limbic system, including the hippocampus (HIP) and amygdala (AMYG); ROIs in the insular cortex (INS); and ROIs in the prefrontal cortex, consisting of the left precentral gyrus (PCG), left middle frontal gyrus (MFG), left medial frontal gyrus (MFG), and ventromedial prefrontal cortical areas (PFCventmed).

In figs. 1 and 2, we show a cortical surface plot of the mean values of ascending or descending BHI coupling strengths respectively that survived false discovery rate multiple corrections for all the frequency bands. The range of connectivity strengths was shown to be lower in descending interactions from the brain to the heart compared to ascending interactions from the heart to the brain. Most significant coupling strengths were observed in the 0.05 Hz to 0.15 Hz band, where ascending interactions preferred the left hemisphere. There were a similar amount of significantly different descending interactions in both hemispheres. The insular cortex highlights interesting results, where the left insula comprised ascending BHI and the right insula comprised descending BHI. In the highest frequency band (0.2 Hz to 0.4 Hz), there were more interactions ascending from the heart to brain than descending from the brain to the heart. Moreover, in low frequencies (0.05 Hz to 0.15 Hz), the brain to heart interactions are primarily negative valued, while in higher frequencies (0.2 Hz to 0.4 Hz) it is positive valued. Negative values in the frequency band of 0.05 Hz to 0.15 Hz indicates brain-heart interactions (measured between BOLD and R-R interval) amplitudes are lesser in high anxiety resting state sessions vs low anxiety sessions. The positive values in the frequency band of 0.2 Hz to 0.4 Hz indicates that brain-heart interactions have increased amplitude in high anxiety resting state sessions as compared to low anxiety sessions.

IV. Discussion and Conclusion

In this study, we describe an fMRI-based methodological framework to assess the different spectral patterns modulating BHI dynamics between high and low anxiety groups entering an MRI scanner. Particularly, we exploited the full frequency directed transfer function (ffDTDF) to glean statistical contrasts between high anxiety and low anxiety groups in the frequency ranges of 0.05 Hz to 0.15 Hz, 0.1 Hz to 0.2 Hz, and 0.2 Hz to 0.4 Hz. From this analysis, we aimed to explore the intricate feedback loops that govern how the brain regulates responses in the heart, and how the heart in return evokes activity in the brain that is instrumental in processing anxiety in an MRI scanner.

We exploited R-R intervals revealed by ECG measurements as a time-varying measure that reflects the complex autonomic activity, then showed how these intervals corresponded to ascending streams of interactions to the brain. We particularly

TABLE I

TABLE OF RESULTS FOR WHICH COUPLING INTERACTIONS BETWEEN HEART AND BRAIN SURVIVED MULTIPLE COMPARISONS CORRECTIONS. THE NUMBERS N OF SIGNIFICANT COMPARISONS ARE INDICATED FOR EACH FREQUENCY BAND, HEMISPHERE AND COUPLING DIRECTION (N = 0, 1, 3, 4, 6, 10, 11, 12, 17, 21 AND 23). ODD ROIS ARE LEFT HEMISPHERE INTERACTIONS WITH THE RRI SIGNALS, WHILE EVEN ROIS ARE RIGHT HEMISPHERE INTERACTIONS WITH THE RRI SIGNALS. OTHER IMPORTANT ROIS IDENTIFIED IN THE WHOLE BRAIN ANALYSIS ARE THE AMYGDALA (41,42), AND THE HIPPOCAMPUS (37,38), THE PRECG (1, 2), THE PFCVENTMED (25, 26), THE MFG (7, 8), THE INS (29, 30), THE ROSTRAL PONS (93, 94, 97, 98) AND THE CAUDAL PONS (105, 106). IN THE HIGH-FREQUENCY BAND (0.2-0.4 HZ), THE HEART DOMINATES THE INTERACTION WITH THE BRAIN IN BOTH HEMISPHERES (N=33 VS. 1), WHILE IN THE LOW-FREQUENCY BAND (0.05-0.15 HZ), THE BRAIN DOMINATES THE INTERACTION WITH THE HEART (N=21 VS. 44)

	Left side		Right side	
	Heart to Brain	Brain to Heart	Heart to Brain	Brain to Heart
0.2 Hz to 0.4 Hz				
N Surviving Connections	12	0	11	1
ROIs	HIP MFG PFCventmed	-	HIP MFG	CER8
0.1 Hz to 0.2 Hz				
N Surviving Connections	10	3	6	4
ROIs	AMYG PreCG PFCventmed **CER9**	CERCRU2 **CER6**	AMYG CER7b **CER10**	
0.05 Hz to 0.15 Hz				
N Surviving Connections	17	23	4	21
ROIs	INS HIP AMYG PreCG PFCventmed CERCRU2 **CER9**	HIP AMYG PFCventmed CERCRU2 **CER4_5** CER8 **CER9**	-	INS CERCRU2 CER7b **CER9**

measured the difference in coupling between high anxiety resting state sessions vs low anxiety sessions of participants in an fMRI scanner. Positive valued results indicated that the ffDTF coupling strength was greater in high anxiety resting state fMRI sessions compared to low anxiety sessions. Otherwise, negative values indicated that low anxiety sessions exhibited higher coupling strength values than high anxiety sessions. This method of analysis can give indicators for specific brain regions that comprise the brain-heart anxiety processing system, with suggestions for whether anxiety increases or decreases ascending (from the heart to the brain) or descending (from the brain to the heart) activity at a certain brain region.

The slurry of significant results ascending from the heart to brain, and descending from the brain to heart, especially after correcting for multiple comparisons, indicates a close bidirectional interaction between body and brain signals during anxiety processing. Of note, as seen in table I, robust coupling was observed between the left upper brainstem/pons ROIs (CER9, CER8, CER4_5) and the cardiac signal (RRI). These results provides additional evidence supporting the hypothesis of a pacemaker-like structure in the pons that generates rhythmic activity at approximately 0.15/0.16 Hz [29], [30]. This finding on its own highlights the potential role of the pons in regulating cardiac function and underscores the complex interplay between brain and body signals during anxiety processing.

Additionally, hippocampus (ROI 37,38) and amygdala (ROI 41,42) were found to be bidirectional between the heart and brain in low frequency interactions, but unidirectional from the heart to the brain in high frequency interactions. Both structures were previously found to be recruited during "fast" nasal breathing in patients with medically intractable epilepsy, and hypothesized to be a by-product of high-anxiety levels [55], [56]. Such a result of this study may give clues to the spectral dynamic of such high and low frequency interactions in the limbic-heart axis of interactions, where low frequency interactions may include cognitive control and bodily feedback of anxiety responses, while high frequencies provide a purely feedforward account of anxiety signalling from the body to the brain.

Twenty ROIs in the AAL2 parcellation (ROIs 91 to 108) were located in the pontine structures in upper brainstem with ROI 109 (corresponding to the vermis 1, 2) most distal and the pair 107, 108 (corresponding to the cerebellum 10). The distance between the BOLD recordings from the pons was approximately 2 mm. From these twenty BOLD signals only 5 survived multiple comparison corrections. The majority of connectivity strengths in frequency in the band 0.1 to 0.2 Hz were small. For example, there were descending brain-heart interactions in high anxiety patients were greater than low anxiety patients in the left brainstem (ROI 93, cerebellum 3) a difference of 0.058. Ascending brain-heart interactions to the left brainstem (ROI 99, cerebellum 7b) were greater in high anxiety patients compared to low anxiety patients with a value difference 0.045. Nonetheless, there were some exceptions; namely large connectivity strengths ($|D_{ji}| > 1$) in connections from heart (RRI) to brain: RRI to left brainstem (ROI 105, cerebellum 10) with -1.18, RRI to right brainstem (ROI 102, cerebellum 8) with -2.07 and RRI to the rostral brainstem (ROI 108, vermis 3) with 1.03.

While ROIs 93, 99 (left cerebellum 3, left cerebellum 7b) are peripheral to the left rostral pons, ROIs 102, 105 and 108 (right cerebellum 8, left cerebellum 10, vermis 3) are localized

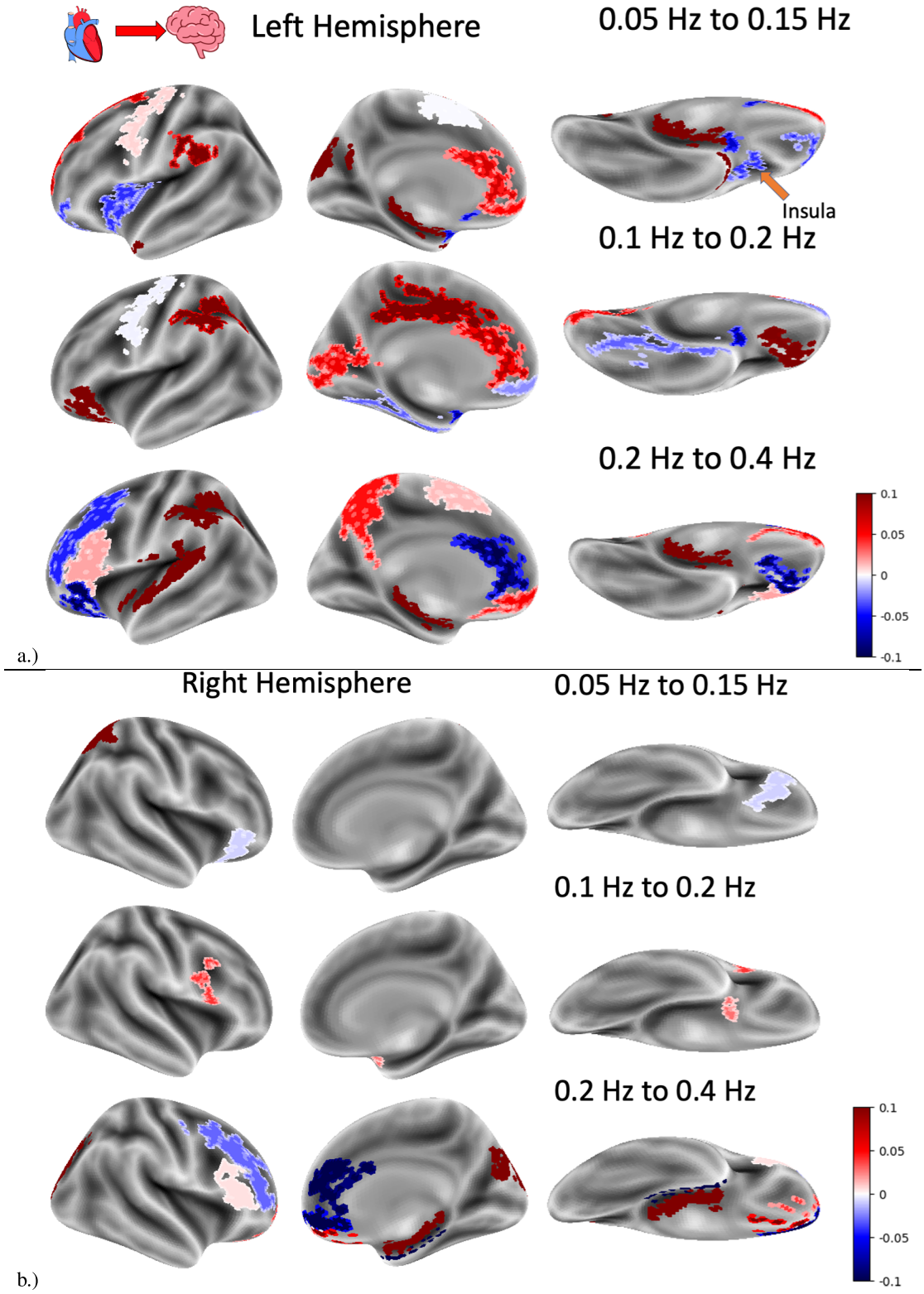

Fig. 1. Cortical surface plots displaying mean difference in ascending connectivity strengths from heart to brain between high and low anxiety participants in the MRI scanner (i.e., the D_{ji} calculated in the statistical analysis) that survived multiple comparisons correction using the false discovery rate procedure. a.) displays the left hemisphere, and b.) displays the results on the right hemisphere. The first column is a lateral view, the middle column is a medial view, and the last column is a ventral view. We show the frequency bands 0.2 Hz to 0.4 Hz (bottom row), 0.1 Hz to 0.2 Hz (middle row) and 0.05 Hz to 0.15 Hz (top row).

near the caudal pons close to the medulla oblongata with the cardiovascular center in lower brainstem. The medullary cardiovascular center is responsible for altering heart rate by sending nerve impulses to the cardiac pacemaker via sympathetic fibers and vagus nerve [37]. It is assumed that the rhythmic electrical activity of this center is accompanied

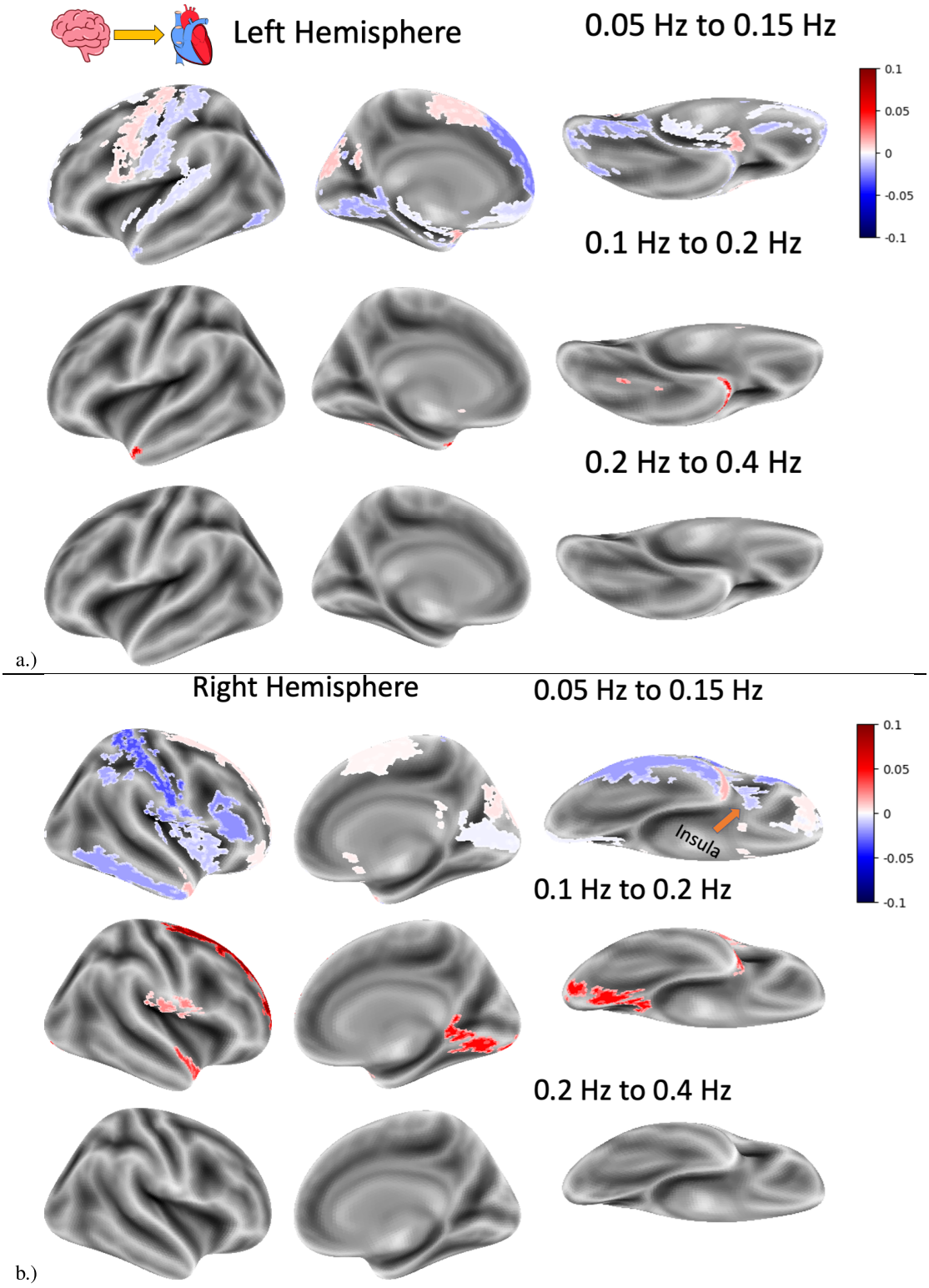

Fig. 2. Cortical surface plots displaying mean difference in descending connectivity strengths from heart to brain between high and low anxiety participants in the MRI scanner (i.e., the D_{ji} calculated in the statistical analysis) that survived multiple comparisons correction using the false discovery rate procedure. a.) displays the left hemisphere, and b.) displays the results on the right hemisphere. The first column is a lateral view, the middle column is a medial view, and the last column is a ventral view. We show the frequency bands 0.2 Hz to 0.4 Hz (bottom row), 0.1 Hz to 0.2 Hz (middle row) and 0.05 Hz to 0.15 Hz (top row).

by a rhythmic BOLD signal focused in the medulla but spreading to the distal part of the pons. This may explain the large coupling between RRI and BOLD signals. In contrast, the descending interactions from brain to heart with small connectivity strengths in ROI 93 (left cerebellum 3) and 99 (left cerebellum 7b) give further support on the existence of a central pacemaker in the rostral pons (centered at ROI 93, left cerebellum 3) modulating the RRI [9], [38].

Of further note, in fig. 1 and fig. 2, we demonstrate the ascending and descending connection strengths respectively, where negative values correspond to the putative system inducing a decreasing response and positive values correspond to a putative system inducing an increasing response in the brain-heart feedback loop. These figures illustrate how fast waves of interaction (0.1 Hz to 0.2 Hz and 0.2 hz to 0.4 Hz) are induced on the heart via the brain stem/pons ROIs, while the cortical structures (such as the insula) suppress (decrease) slow waves (0.05 Hz to 0.15 Hz) amplitudes in the heart rate. This even further highlights the evidence of the pacemaker/regulator function descending from the brain stem to the heart in anxiety processing and while demonstrating the role of cortical structures like the insula in cognitive control [29], [30], [39].

Beyond the pacemaker aspect, our findings indicate the presence of ascending information transfer from the heart to the left insula and descending information transfer from the right insula to the heart in the low frequency band (0.05-0.15 Hz). This supports the concept of hemispheric differences in ascending and descending brain-body interplay during anxiety processing, as previously reported in [8]. These results suggest that the insula plays a critical role in integrating cardiac and neural signals and highlights the importance of bidirectional communication between the brain and body in the context of anxiety and cognitive control. In fact, the heart induces higher activity across the neocortex, especially in the ventromedial prefrontal cortical areas such as the inferior orbital cortex and middle frontal gyrus. This can suggest that the heart is actually invoking cognitive control for anxiety processing. This is indeed in line with recent literature regarding the heart's role in eliciting emotional responses [57]. In general, ascending interactions from the heart to the brain preferred left hemispheric interactions, although at higher frequencies the right hemisphere starts to be affected by the heart intervals, with a similar amount of significantly different connections between groups found in the 0.2 Hz to 0.4 Hz frequency band.

A caveat of the current analysis is that although we measured interaction differences between participants undergoing low and high levels of anxiety, the differential strength measure does not give any indicators for whether the increase or decrease in coupling strength reflects in a possible change from excitatory to inhibitory interactions or vice-versa. This kind of analysis would comprise an assessment whether the increase or decrease in coupling strength also comprises a zero-crossing. For example, a pontine structure's interaction with the heart may be an effectively null or negative interaction during low-anxiety sessions, but crosses into a positive coupling interaction when the participant is exhibiting high levels of anxiety. Thus, future analyses of similar datasets may attempt to perform robust statistics to infer such phenomena.

The STADI was used for categorization of participants in low and high anxiety states in the fMRI scanner. This measure has been shown as a standard and reliable method to evaluate anxiety. However, our analysis does not take into consideration potential factors such as fatigue or drowsiness that could be argued to affect regulation of the brain-heart axis. Nonetheless, we maintain the validity of this analysis given the attentiveness of the participants to respond to the STADI inventory effectively to demonstrate distinct low and high anxiety states in different sessions. Furthermore, such aspects can instead be reflections of low-anxiety, with the participant becoming relaxed during the study [60].

This study focused on three bands of interest, and their physiological significance has been steadily growing in the literature. Since the work of Perlitz et al., 2004 [61], paper by Keller et al., 2020 [62], we have evidence suggesting the existence of an intermediate band (IM: 0.12-0.18 Hz) related to interoceptive perception. The origin of this IM band may be located in the brainstem and be a part of the reticular system capable of generating rhythmic activity with a center frequency at around 0.15/0.16 Hz. Such a pacemaker in the brainstem is also active during the processing of negative emotions [30]. BOLD spectra often display two power peaks around 0.1 Hz. One peak, with a frequency less than 0.1 Hz, represents the vascular BOLD, while the other peak, with a frequency greater than 0.1 Hz, represents the neural BOLD component. The vascular component of the BOLD signal could be separated from the neural oscillations based on their timing, with the former clearly preceding the latter [16].

On this note, it is worth mentioning that analyses were performed directly on the BOLD signal rather than using a deconvolutional approach of connectivity [58]. Indeed, such approaches are crucial when assessing interactions between within cortical components of the brain, as connectivity effects may be confounded by the sluggish nature of the BOLD signal with non-constant time-delays between the neural signal and the BOLD signal [59]. However, we wish to point out that such literature is specific for connectivity between brain areas where the effects of hemodynamics wish to be regressed out of the equations, and not for brain-heart interactions. However, as [16] has shown, there are distinct components of the BOLD signals that correspond various cardiac effects in our frequencies of interest. Thus, we contend that a deconvolutional approach could hamper interpretation of the results, as brain-heart interactions may comprise effects which may reflect in local variations of the hemodynamic response. Nonetheless, we encourage future studies to intricately assess the effects of the heart rate variability on the hemodynamic response, and subsequently their effects on the latent neural signals.

We would like to further elaborate on the interactions between the amygdala and hippocampus in relation to high-frequency brain-heart dynamics (ranging from 0.1 Hz to 0.4 Hz). The amygdala and hippocampus play pivotal roles in regulating fear and anxiety responses [63]. Our investigation revealed a notable pattern: interactions predominantly involve the amygdala within the 0.1 Hz to 0.2 Hz range, whereas hippocampal involvement is more pronounced within the 0.2 Hz to 0.4 Hz range. Extensive literature has clarified the distinct functions of these regions, with the hippocampus primarily involved in approach-avoidance value computations and the amygdala focused on fear processing [64]. On a speculative note, our findings suggest that amygdala activity may correspond to fear-induced responses triggered by entering the MRI machine, whereas hippocampal engagement may relate to the evaluation of avoidance strategies while

actively undergoing MRI scanning. However, it is imperative to conduct further experimental manipulations to validate these interpretations. Future studies should incorporate control measures to further elucidate the frequency-dependent dynamics within the amygdala-hippocampal circuitry underlying fear and anxiety.

V. Conclusion

Our study delves into the spectral dynamics between the heart and brain during anxiety processing while participants undergo MRI scans. We observe a pacemaking function originating from the brainstem, eliciting cardiac responses, aligning with existing literature detailing the neuroanatomy of cardiogenic control. Additionally, our findings indicate that the heart plays a pivotal role in eliciting cortical activity in the prefrontal cortex associated with cognitive control. Moreover, we identify hemispheric ascending and descending streams of brain-heart interactions mediated by the insular cortex.

These results hold significant implications for enhancing our comprehension and potential management of anxiety factors frequently encountered in psychological experiments conducted within MRI scanners. Furthermore, they shed light on the intricate feedback loops between the brain and heart that underpin anxiety disorders.

Acknowledgment

The authors would like to thank David Fink for support in data acquisition, Clemens Brunner for support in data processing, and Andreas Schwerdtfeger for evaluations of state anxiety (all of them from University of Graz).

References

[1] M. M. Kenwood, N. H. Kalin, and H. Barbas, "The prefrontal cortex, pathological anxiety, and anxiety disorders," *Neuropsychopharmacology*, vol. 47, no. 1, pp. 260–275, Jan. 2022.

[2] M. G. Craske, S. L. Rauch, R. Ursano, J. Prenoveau, D. S. Pine, and R. E. Zinbarg, "What is an anxiety disorder?" *Focus*, vol. 9, no. 3, pp. 369–388, 2011.

[3] B. Martin, "The assessment of anxiety by physiological behavioral measures," *Psychol. Bull.*, vol. 58, no. 3, pp. 234–255, May 1961.

[4] B. F. Fuller, "The effects of stress-anxiety and coping styles on heart rate variability," *Int. J. Psychophysiol.*, vol. 12, no. 1, pp. 81–86, Jan. 1992.

[5] R. Jerath, M. W. Crawford, V. A. Barnes, and K. Harden, "Self-regulation of breathing as a primary treatment for anxiety," *Appl. Psychophysiol. Biofeedback*, vol. 40, no. 2, pp. 107–115, Jun. 2015.

[6] R. Hoehn-Saric and D. R. McLeod, "Anxiety and arousal: Physiological changes and their perception," *J. Affect. Disorders*, vol. 61, no. 3, pp. 217–224, Dec. 2000.

[7] E. A. Wehrwein, H. S. Orer, and S. M. Barman, "Overview of the anatomy, physiology, and pharmacology of the autonomic nervous system," *Regulation*, vol. 37, no. 69, p. 125, 2016.

[8] A. D. Craig, "Forebrain emotional asymmetry: A neuroanatomical basis?" *Trends Cognit. Sci.*, vol. 9, no. 12, pp. 566–571, Dec. 2005.

[9] G. Pfurtscheller et al., "Brain-heart communication: Evidence for 'central pacemaker' oscillations with a dominant frequency at 0.1 Hz in the cingulum," *Clin. Neurophysiol.*, vol. 128, no. 1, pp. 183–193, 2017.

[10] F. Malandrone et al., "Restoring bottom-up communication in brain-heart interplay after trauma-focused psychotherapy in breast cancer patients with post-traumatic stress disorder," *J. Affect. Disorders*, vol. 351, pp. 143–150, Apr. 2024.

[11] V. Catrambone, L. Zallocco, E. Ramoretti, M. R. Mazzoni, L. Sebastiani, and G. Valenza, "Integrative neuro-cardiovascular dynamics in response to test anxiety: A brain-heart axis study," *Physiol. Behav.*, vol. 276, Mar. 2024, Art. no. 114460.

[12] G. Pfurtscheller, A. R. Schwerdtfeger, B. Rassler, A. Andrade, and G. Schwarz, "MRI-related anxiety can induce slow BOLD oscillations coupled with cardiac oscillations," *Clin. Neurophysiol.*, vol. 132, no. 9, pp. 2083–2090, Sep. 2021.

[13] K. J. Murphy and J. A. Brunberg, "Adult claustrophobia, anxiety and sedation in MRI," *Magn. Reson. Imag.*, vol. 15, no. 1, pp. 51–54, Jan. 1997.

[14] J. C. Meléndez, "Anxiety-related reactions associated with magnetic resonance imaging examinations," *JAMA, J. Amer. Med. Assoc.*, vol. 270, no. 6, pp. 745–747, Aug. 1993.

[15] X. V. Nguyen et al., "Prevalence and financial impact of claustrophobia, anxiety, patient motion, and other patient events in magnetic resonance imaging," *Topics Magn. Reson. Imag.*, vol. 29, no. 3, pp. 125–130, 2020.

[16] S. Tumati, M. P. Paulus, and G. Northoff, "Out-of-step: Brain-heart desynchronization in anxiety disorders," *Mol. Psychiatry*, vol. 26, no. 6, pp. 1726–1737, Jun. 2021.

[17] B. M. Appelhans and L. J. Luecken, "Heart rate variability as an index of regulated emotional responding," *Rev. Gen. Psychol.*, vol. 10, no. 3, pp. 229–240, Sep. 2006.

[18] J. A. Chalmers, D. S. Quintana, M. J.-A. Abbott, and A. H. Kemp, "Anxiety disorders are associated with reduced heart rate variability: A meta-analysis," *Frontiers Psychiatry*, vol. 5, p. 80, Jul. 2014.

[19] J. M. Gorman and R. P. Sloan, "Heart rate variability in depressive and anxiety disorders," *Amer. Heart J.*, vol. 140, no. 4, pp. 77–83, Oct. 2000.

[20] M. Davis, "The role of the amygdala in fear and anxiety," *Annu. Rev. Neurosci.*, vol. 15, no. 1, pp. 353–375, Jan. 1992.

[21] O. Babaev, C. Piletti Chatain, and D. Krueger-Burg, "Inhibition in the amygdala anxiety circuitry," *Experim. Mol. Med.*, vol. 50, no. 4, pp. 1–16, Apr. 2018.

[22] J. J. Wong, N. M. L. Wong, D. H. F. Chang, D. Qi, L. Chen, and T. M. C. Lee, "Amygdala–pons connectivity is hyperactive and associated with symptom severity in depression," *Commun. Biol.*, vol. 5, no. 1, p. 574, Jun. 2022.

[23] A. K. Anderson and E. A. Phelps, "Lesions of the human amygdala impair enhanced perception of emotionally salient events," *Nature*, vol. 411, no. 6835, pp. 305–309, May 2001.

[24] I. Liberzon, K. L. Phan, L. R. Decker, and S. F. Taylor, "Extended amygdala and emotional salience: A PET activation study of positive and negative affect," *Neuropsychopharmacology*, vol. 28, no. 4, pp. 726–733, Apr. 2003.

[25] P. R. Koehler et al., "MR measurement of normal and pathologic brainstem diameters," *Amer. J. Neuroradiol.*, vol. 6, no. 3, pp. 425–427, 1985.

[26] T. E. Dick, D. M. Baekey, J. F. R. Paton, B. G. Lindsey, and K. F. Morris, "Cardio-respiratory coupling depends on the pons," *Respiratory Physiol. Neurobiol.*, vol. 168, nos. 1–2, pp. 76–85, Aug. 2009.

[27] P. J. Davern, "A role for the lateral parabrachial nucleus in cardiovascular function and fluid homeostasis," *Frontiers Physiol.*, vol. 5, p. 436, Nov. 2014.

[28] G. Pfurtscheller, K. J. Blinowska, M. Kaminski, B. Rassler, and W. Klimesch, "Processing of fMRI-related anxiety and information flow between brain and body revealed a preponderance of oscillations at 0.15/0.16 Hz," *Sci. Rep.*, vol. 12, no. 1, p. 9117, Jun. 2022.

[29] G. Pfurtscheller et al., "Processing of fMRI-related anxiety and bi-directional information flow between prefrontal cortex and brain stem," *Sci. Rep.*, vol. 11, no. 1, p. 22348, Nov. 2021.

[30] G. Pfurtscheller, A. R. Schwerdtfeger, B. Rassler, A. Andrade, G. Schwarz, and W. Klimesch, "Verification of a central pacemaker in brain stem by phase-coupling analysis between HR interval-and BOLD-oscillations in the 0.10–0.15 Hz frequency band," *Frontiers Neurosci.*, vol. 14, p. 922, Aug. 2020.

[31] L. A. Schwarz and L. Luo, "Organization of the locus coeruleus-norepinephrine system," *Current Biol.*, vol. 25, no. 21, pp. 1051–1056, Nov. 2015.

[32] A. Grimonprez et al., "The antidepressant-like effect of vagus nerve stimulation is mediated through the locus coeruleus," *J. Psychiatric Res.*, vol. 68, pp. 1–7, Sep. 2015.

[33] D. R. Hulsey, J. R. Riley, K. W. Loerwald, R. L. Rennaker, M. P. Kilgard, and S. A. Hays, "Parametric characterization of neural activity in the locus coeruleus in response to vagus nerve stimulation," *Experim. Neurol.*, vol. 289, pp. 21–30, Mar. 2017.

[34] J. M. Thornton, T. Aziz, D. Schlugman, and D. J. Paterson, "Electrical stimulation of the midbrain increases heart rate and arterial blood pressure in awake humans," *J. Physiol.*, vol. 539, no. 2, pp. 615–621, Mar. 2002.

[35] M. L. Brandão, S. H. Cardoso, L. L. Melo, V. Motta, and N. C. Coimbra, "Neural substrate of defensive behavior in the midbrain tectum," *Neurosci. Biobehavioral Rev.*, vol. 18, no. 3, pp. 339–346, Sep. 1994.

[36] V. C. Goessl, J. E. Curtiss, and S. G. Hofmann, "The effect of heart rate variability biofeedback training on stress and anxiety: A meta-analysis," *Psychol. Med.*, vol. 47, no. 15, pp. 2578–2586, Nov. 2017.

[37] J. Ciriello, M. Caverson, and C. Polosa, "Function of the ventrolateral medulla in the control of the circulation," *Brain Res. Rev.*, vol. 11, pp. 259–291, Dec. 2023.

[38] G. Pfurtscheller, M. Kaminski, K. J. Blinowska, B. Rassler, G. Schwarz, and W. Klimesch, "Respiration-entrained brain oscillations in healthy fMRI participants with high anxiety," *Sci. Rep.*, vol. 13, no. 1, p. 2380, Feb. 2023.

[39] B. Hsueh et al., "Cardiogenic control of affective behavioural state," *Nature*, vol. 615, no. 7951, pp. 292–299, Mar. 2023.

[40] A. D. Craig, "How do you feel? Interoception: The sense of the physiological condition of the body," *Nature Rev. Neurosci.*, vol. 3, no. 8, pp. 655–666, Aug. 2002.

[41] Z. Munn, S. Moola, K. Lisy, D. Riitano, and F. Murphy, "Claustrophobia in magnetic resonance imaging: A systematic review and meta-analysis," *Radiography*, vol. 21, no. 2, pp. 59–63, May 2015.

[42] H. A. Chapman, D. Bernier, and B. Rusak, "MRI-related anxiety levels change within and between repeated scanning sessions," *Psychiatry Res., Neuroimaging*, vol. 182, no. 2, pp. 160–164, May 2010.

[43] M. Mather and J. F. Thayer, "How heart rate variability affects emotion regulation brain networks," *Current Opinion Behav. Sci.*, vol. 19, pp. 98–104, Feb. 2018.

[44] A. Korzeniewska, M. Mańczak, M. Kamiński, K. J. Blinowska, and S. Kasicki, "Determination of information flow direction among brain structures by a modified directed transfer function (dDTF) method," *J. Neurosci. Methods*, vol. 125, nos. 1–2, pp. 195–207, 2003.

[45] C. W. J. Granger, "Investigating causal relations by econometric models and cross-spectral methods," *Econometrica*, vol. 37, no. 3, pp. 424–438, Aug. 1969.

[46] M. J. Kaminski and K. J. Blinowska, "A new method of the description of the information flow in the brain structures," *Biol. Cybern.*, vol. 65, no. 3, pp. 203–210, Jul. 1991.

[47] E. T. Rolls, M. Joliot, and N. Tzourio-Mazoyer, "Implementation of a new parcellation of the orbitofrontal cortex in the automated anatomical labeling atlas," *NeuroImage*, vol. 122, pp. 1–5, Nov. 2015.

[48] R. K. Niazy, C. F. Beckmann, G. D. Iannetti, J. M. Brady, and S. M. Smith, "Removal of FMRI environment artifacts from EEG data using optimal basis sets," *NeuroImage*, vol. 28, no. 3, pp. 720–737, Nov. 2005.

[49] M. P. Tarvainen, J.-P. Niskanen, J. A. Lipponen, P. O. Ranta-Aho, and P. A. Karjalainen, "Kubios HRV–heart rate variability analysis software," *Comput. Methods Programs Biomed.*, vol. 113, no. 1, pp. 210–220, 2014.

[50] G. Pfurtscheller et al., "Synchronization of intrinsic 0.1-Hz blood-oxygen-level-dependent oscillations in amygdala and prefrontal cortex in subjects with increased state anxiety," *Eur. J. Neurosci.*, vol. 47, no. 5, pp. 417–426, Mar. 2018.

[51] S. Moeller et al., "Multiband multislice GE-EPI at 7 Tesla, with 16-fold acceleration using partial parallel imaging with application to high spatial and temporal whole-brain fMRI," *Magn. Reson. Med.*, vol. 63, no. 5, pp. 1144–1153, May 2010.

[52] B. P. Rogers, S. B. Katwal, V. L. Morgan, C. L. Asplund, and J. C. Gore, "Functional MRI and multivariate autoregressive models," *Magn. Reson. Imag.*, vol. 28, no. 8, pp. 1058–1065, Oct. 2010.

[53] C. Chang and G. H. Glover, "Time–frequency dynamics of resting-state brain connectivity measured with fMRI," *NeuroImage*, vol. 50, no. 1, pp. 81–98, Mar. 2010.

[54] Y. Benjamini and Y. Hochberg, "Controlling the false discovery rate: A practical and powerful approach to multiple testing," *J. Royal Stat. Soc. Ser. B*, vol. 57, no. 1, pp. 289–300, Jan. 1995.

[55] C. Zelano et al., "Nasal respiration entrains human limbic oscillations and modulates cognitive function," *J. Neurosci.*, vol. 36, no. 49, pp. 12448–12467, Dec. 2016.

[56] J. L. Herrero, S. Khuvis, E. Yeagle, M. Cerf, and A. D. Mehta, "Breathing above the brain stem: Volitional control and attentional modulation in humans," *J. Neurophysiol.*, vol. 119, no. 1, pp. 145–159, Jan. 2018.

[57] D. Candia-Rivera, V. Catrambone, J. F. Thayer, C. Gentili, and G. Valenza, "Cardiac sympathetic-vagal activity initiates a functional brain–body response to emotional arousal," *Proc. Nat. Acad. Sci. USA*, vol. 119, no. 21, May 2022, Art. no. e2119599119.

[58] D. R. Gitelman, W. D. Penny, J. Ashburner, and K. J. Friston, "Modeling regional and psychophysiologic interactions in fMRI: The importance of hemodynamic deconvolution," *NeuroImage*, vol. 19, no. 1, pp. 200–207, May 2003.

[59] G. Deshpande, K. Sathian, and X. Hu, "Effect of hemodynamic variability on Granger causality analysis of fMRI," *NeuroImage*, vol. 52, no. 3, pp. 884–896, Sep. 2010.

[60] G. M. Manzoni, F. Pagnini, G. Castelnuovo, and E. Molinari, "Relaxation training for anxiety: A ten-years systematic review with meta-analysis," *BMC Psychiatry*, vol. 8, no. 1, pp. 1–12, Dec. 2008.

[61] V. Perlitz et al., "Coordination dynamics of circulatory and respiratory rhythms during psychomotor drive reduction," *Autonomic Neurosci.*, vol. 115, nos. 1–2, pp. 82–93, Sep. 2004.

[62] M. Keller et al., "Neural correlates of fluctuations in the intermediate band for heart rate and respiration are related to interoceptive perception," *Psychophysiology*, vol. 57, no. 9, Sep. 2020, Art. no. e13594.

[63] P. Tovote, J. P. Fadok, and A. Lüthi, "Neuronal circuits for fear and anxiety," *Nature Rev. Neurosci.*, vol. 16, no. 6, pp. 317–331, Jun. 2015.

[64] D. M. Bannerman et al., "Regional dissociations within the hippocampus—Memory and anxiety," *Neurosci. Biobehavioral Rev.*, vol. 28, no. 3, pp. 273–283, May 2004.

Open Access funding provided by 'Università di Pisa' within the CRUI CARE Agreement